Circularly polarized light emission from chiral spatially-structured planar semiconductor microcavities

A. A. Maksimov,[1] I. I. Tartakovskii,[1] E. V. Filatov,[1] S. V. Lobanov,[2,3] N. A. Gippius,[3] S. G. Tikhodeev,[3,2,*] C. Schneider,[4] M. Kamp,[4] S. Maier,[4] S. Höfling,[4] and V. D. Kulakovskii[1]

[1]*Institute of Solid State Physics, Russian Academy of Science, Chernogolovka 142432, Russia*

[2]*M. V. Lomonosov Moscow State University, Moscow, Russia*

[3]*A. M. Prokhorov General Physics Institute, Russian Academy of Science, Moscow, Russia*

[4]*Technische Physik and Wilhelm-Conrad-Röntgen-Research Center for Complex Material Systems, Universität Würzburg, D-97074 Würzburg, Am Hubland, Germany*

(Received 8 October 2013; revised manuscript received 17 January 2014; published 31 January 2014)

We demonstrate a method for control of the polarization of emission of quantum dots (QDs) embedded in an active layer of a planar microcavity. This method involves a modification of the electromagnetic mode structure in a planar microcavity which is achieved by fabrication of a chiral gammadion layer structure with partial etching of the upper Bragg mirror. A polarization degree as high as 81% has been demonstrated experimentally without the use of a static magnetic field or birefringent wave plates; this is in full agreement with the theoretical simulations for the fabricated structure. Theoretical optimization has shown that a polarization degree of up to 99% can be achieved in optimized structures with randomly positioned quantum dots, and to an even higher degree when the QDs have controlled positions.

DOI: 10.1103/PhysRevB.89.045316 PACS number(s): 78.67.Pt, 42.25.Ja, 42.50.Pq, 81.05.Xj

Polarization conversion and rotation are usually realized with the use of wave plates of birefringent materials and optical gratings. Advances in nano- and microscale fabrication have made it possible to realize artificial materials (photonic structures and/or metamaterials) with extraordinary optical properties. The polarization and intensity of the light emitted from a photonic structure depends on the internal structure of the source as well as the symmetry and density of the environmentally allowed electromagnetic modes. Modification of the mode structure relative to that in free space affects the spontaneous emission rate of emitted light and its radiation pattern and direction [1–3]. The role of the latter is most pronounced in the case of a light emitter in a microcavity [4,5]. An imbalance between the left- and right-circularly polarized photons in semiconductors is usually reached by applying a static magnetic field, resulting in splitting of the left- and right-circularly polarized modes due to disturbance of the time-reversal symmetry. A strong imbalance between the left- and right-circularly polarized photons may also occur in chiral materials with nonequivalent left- and right-circularly polarized electromagnetic field modes [6] .

Note however that polarization effects are qualitatively determined by the overall symmetry of a sample [7], not the details of how this symmetry arises. Recently it has been shown that plasmonic structures and/or metamaterials exhibit extraordinary capabilities in controlling and manipulating the polarization states of light. For example, 2D arrays of planar chiral structures of gammadion-shaped metal nanoparticles or nanoapertures produced by broken front-back symmetry exhibit a large circular dichroism and a giant optical activity [8], exceeding significantly those of conventional three-dimensional materials. Optical activity with an extraordinary rotational power was also observed in a planar dielectric waveguide coupled to a dielectric chiral sub-wavelength-period grating [9]. Circularly polarized light emission with a polarization degree ρ_c of 26% has been obtained from InAs quantum dots (QDs) embedded in the waveguide region of such a GaAs-based nanostructure [6]. The helicity of emission was opposite for the structures with left- and right-twisted gammadions, and was absent prior to gammadion etching.

In this paper, we propose a type of planar high quality factor semiconductor microcavity (MC) with QDs embedded in the active region and chiral modulation of the upper mirror which enables us to control effectively the polarization of QDs light emission. The circular polarization degree of InAs QD emission as high as 0.81 is experimentally realized in fabricated GaAs-based semiconductor MCs with an incorporated InAs QD layer and a gammadion layer structure etched through the half of the upper Bragg mirror. Thus, the considered chiral structure fabricated from conventional achiral semiconductor materials using the chiral morphology effect offers important fundamental insights and also enables the creation of solid-state circularly polarized light-emitting devices with the use of the state-of-the-art semiconductor fabrication processes. Moreover, we demonstrate by a numerical simulation that the imbalance between the left- and right-circularly polarized vacuum electromagnetic modes in such MC opens a way to designing light emitters (including single photon emitters in case of the precise control of a single QD emitter position) with nearly 100% degree of circular polarization at zero magnetic field.

A chiral photonic crystal is fabricated from the GaAs-based MC grown by molecular beam epitaxy on a GaAs substrate. The full planar cavity consists of 23.5/20 pairs of AlAs/GaAs layers in the lower/upper Bragg reflectors and a GaAs active layer with an incorporated InAs QD layer. The nominal thicknesses of the AlAs and GaAs layers in Bragg mirrors are 80 nm and 69 nm, respectively. The thickness of the cavity layer is 261 nm, the QD density is equal to 20 μm^{-2}. A gammadion layer is fabricated by nanolithography and dry etching of 10 pairs of GaAs/AlAs layers of the upper mirror. Representative SEM pictures of the chiral photonic layer are shown in Fig. 1.

*tikh@gpi.ru

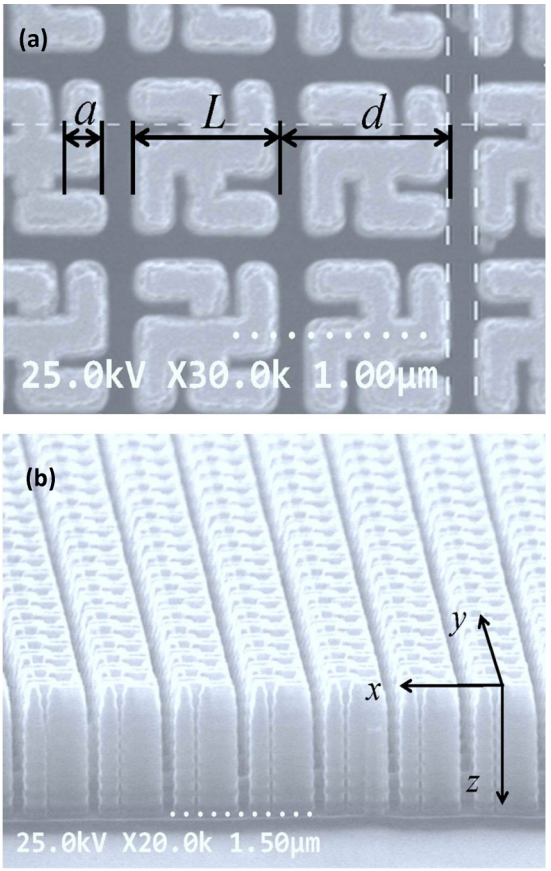

FIG. 1. (Color online) Representative scanning electron microscopy (SEM) pictures of the chiral photonic crystal fabricated from GaAs-based MC, top (a) and side (b) view. The period of the structure, the gammadion size, and linewidth are d, L, and a, respectively.

It consists of gammadion pillars that have a broken in-plane mirror symmetry but possess a fourfold rotational axis and are expected to demonstrate a strong optical activity [9].

A set of $400 \times 400\ \mu\text{m}^2$ chiral fields is fabricated on the same planar MC. The lateral gammadion size L varies from 2 μm down to 400 nm. The gammadion linewidth is $a \sim 0.26L$. The samples are held at a temperature of 5 K in the insert of an optical cryostat. For optical excitation we use a semiconductor laser with a wavelength of 630 nm. The laser spot has a diameter of about 10 μm; the laser power incident on the sample is limited to 20 mW. The emission is dispersed by a monochromator and detected by a LN_2-cooled Si charge-coupled-devices camera. The polarization of the luminescence is analyzed by a quarter wave retarder and linear polarizers. The angle resolution of 0.5° is ensured by a small aperture. The circular polarization degree of the luminescence from the MC prior to etching is less than 1%.

Figures 2(a) and 2(b) display the measured polarized emission spectra from the MC areas with right- (H4) and left-twisted (C4) gammadions recorded at the normal to the MC plane at zero magnetic field in the spectral range near the ground cavity state. The gammadion size and period are 750 and 1290 nm, respectively. The spectra demonstrate a narrow line with the same photon energy but different intensities in

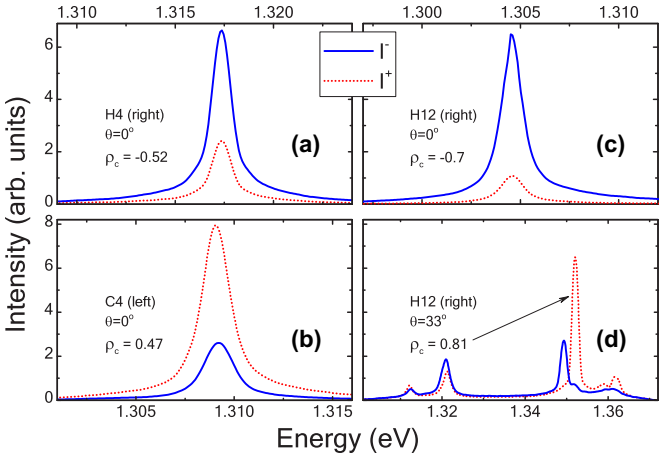

FIG. 2. (Color online) Measured emission spectra of gammadions with size/period 750/1290 (a),(b) and 400/1000 nm (c),(d). The gammadions are right-twisted [as shown in Fig. 1(a)] in panels (a),(c),(d) and left-twisted in panel (b). Note that the helicity of emission is opposite in panels (a) and (b). The measured circular polarization degree reaches 70% and 81% in panels (c) and (d), respectively.

the right (I^+) and left (I^-) circular polarizations. The degrees of circular polarization

$$\rho_c = \frac{I^+ - I^-}{I^+ + I^-} \tag{1}$$

are equal to $+0.52$ and -0.47 ± 0.02 for the fields with left- and right-twisted gammadions, respectively. The opposite helicity of the emission from the fields with opposite gammadion orientations proves that the gammadion layers fabricated on top of the planar semiconductor MC make the compound structure chiral.

More detailed measurements of ρ_c from the gammadion fields with various gammadion sizes L and ratios L/d have shown that $|\rho_c|$ is not a monotonic function of both L and L/d. Thus, in the interval 400 nm $\leqslant L \leqslant$ 1000 nm the maximum ρ_c does not exceed 0.3 for the fields with a high gammadion density ($L/d = 5/6$). To obtain a higher value of ρ_c one has to increase the space between the gammadions. The maximum values of ρ_c at $\theta = 0$ are obtained at the fields with $L = 700 \pm 50$ nm and $L/d \sim 0.6$ where $|\rho_c|$ is in the range of 0.45 ± 0.05 [Figs. 2(a) and 2(b)] and at the fields with $L \sim 400$ nm and $L/d \sim 0.4$ where $|\rho_c|$ reaches 0.7 [Fig. 2(c)].

Figures 3(a) and 3(b) show (in the semilog scale) an angular distribution of the σ^+ and σ^- components of cavity emission in a wide spectral range for H4 field with right-twisted gammadions ($d = 1000$ nm, $L = 400$ nm, $a \sim 100$ nm). The components in panels (a) and (b) are recorded at $k_y = 0$ under the same excitation condition as in Fig. 2. For clarity they are normalized at each angle on the integral intensity at this angle. First, it is seen that the periodic gammadion structure in the x direction results in folding of the cavity mode in the k_x direction with a period of $k_x = 2\pi/d$. The periodic gammadion structure in the y direction results in folding of the cavity mode in the k_y direction with the same period $k_y = 2\pi/d$. These folded modes are shifted to the high energy side. In what follows we label the dispersion branches of

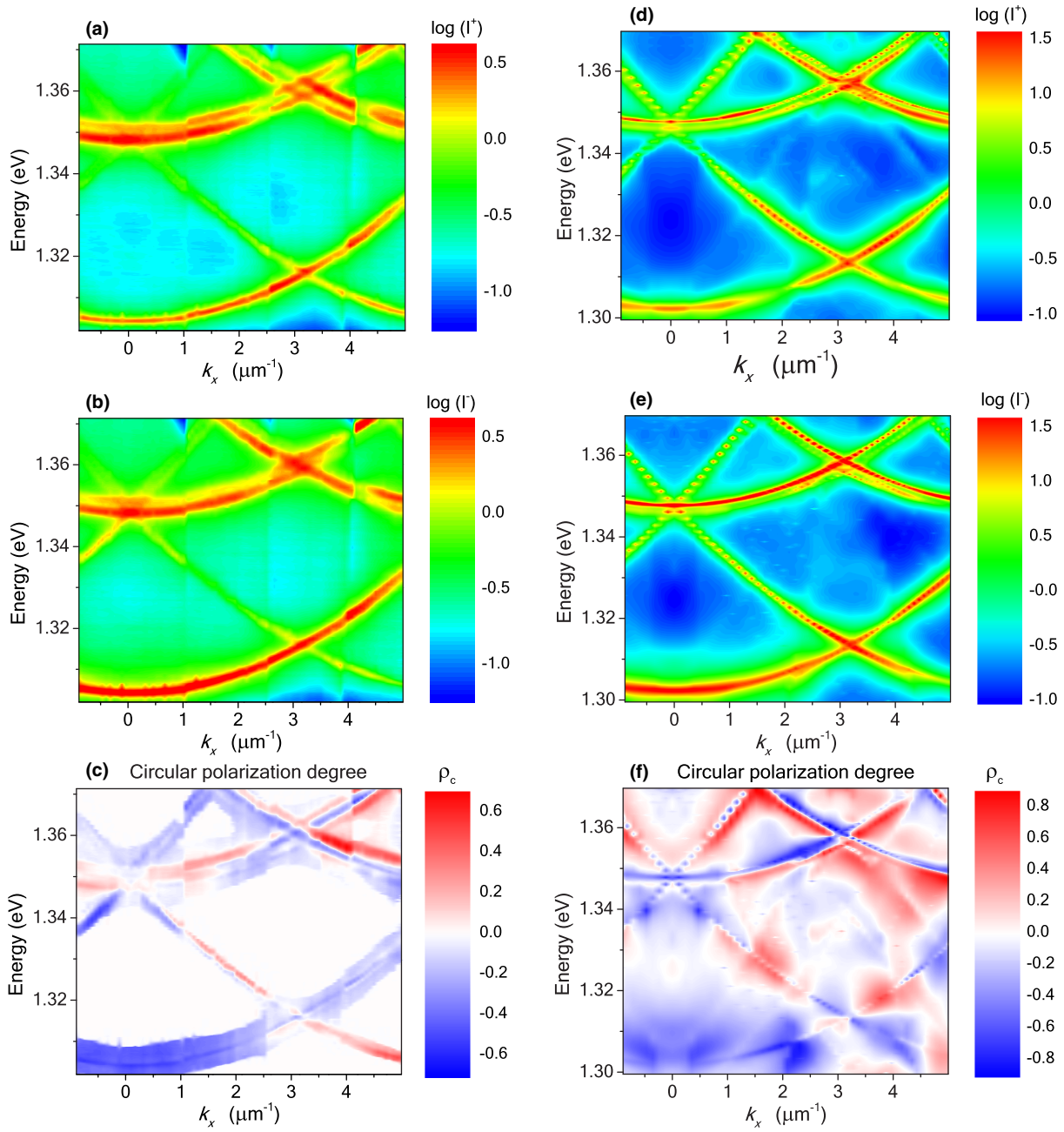

FIG. 3. (Color online) Measured [panels (a),(b)] and calculated (d),(e) angular dependencies of QD emission intensity in σ^+ and σ^- polarizations (top and middle panels, respectively); measured (c) and calculated (f) circular polarization of emission. The experimental spectra were recorded for right-twisted gammadions (field H12, $d = 1000$ nm, $L = 400$ nm, and $a \sim 100$ nm). The theoretical spectra were calculated for the right-twisted gammadions with the same d, L, $a = 103$ nm, and 10 etched Bragg pairs of the top mirror.

the modes as (i, j), where i and j stand for the numbers of the branch folding in the k_x and k_y directions, respectively. As expected, branches $(0,\pm1)$ and $(\pm1,0)$ have the same energy at $k_x = k_y = 0$ due to the same periods in the x and y directions. No marked mode anticrossing is observed, which is in agreement with a negligible cavity mode coupling. At large k the modes split into doublets, which is related to the TE-TM splitting of the planar cavity mode [10].

Figure 3(c) shows that the measured ρ_c of the emission of all the modes depends on k; even the sign of ρ_c is not constant. Moreover, it is seen in Fig. 3(c) that the maximum values of positive and negative ρ_c for modes $(0,0)$ at $k \sim 0$ and $(1,1)$ at $\mathbf{k} = \{\sim 3.5, 0\}\ \mu\text{m}^{-1}$, respectively, are very similar, $|\rho_c| \sim 0.7$. Note, however, that the helicity of the emission from fields with the right- and left-twisted gammadions is opposite for all modes (not shown). Finally, it is also worth noting that the maximum ρ_c in the field H12, $\rho_c = 0.81$, was obtained for the mode $(1,1)$ at $\theta = 33^\circ$ corresponding to $\mathbf{k} = \{3.4, 0.5\}\ \mu\text{m}^{-1}$. This is illustrated in Fig. 2(d).

A reasonable approach to calculate the QD emission from a photonic structure is to describe the QDs as a set of linearly polarized point dipoles distributed and oriented randomly in

the MC active layer. Each dipole is assumed to have a point current $\mathbf{j}(\mathbf{r},t) = \mathbf{j}_0\delta(\mathbf{r}-\mathbf{r}_0)e^{-i\omega t}$ with amplitude $\mathbf{j}_0$ fixed by an external source, the so-called weak coupling limit. The emission intensity as a function of oscillation frequency and direction can be then calculated with accounting for the modulated dielectric surrounding using the optical scattering matrix approach [11–14]. However, we use the electrodynamic reciprocity principle [15] to simplify the simulation. According to this principle the currents of two different dipoles $\mathbf{j}_{1,2}$ and their electric fields $\mathbf{E}_{1,2}$ at the positions of the another dipole are connected,

$$\mathbf{j}_1\mathbf{E}_2 = \mathbf{j}_2\mathbf{E}_1. \tag{2}$$

This enables us to calculate the $\sigma^{\pm}$ circularly polarized components of the emission fields $\mathbf{E}_1^{\pm}$ of each linearly (in the xy plane) polarized QD with $\mathbf{j}_1 \propto \vec{e}_{x,y}$ in the far field zone. Namely, we have to calculate the local fields at the position of QD $\mathbf{E}_2^{\mp} = E_2^{\mp}\vec{e}_{x,y}$ of a $\sigma^{\mp}$-circularly polarized dipole $\mathbf{j}_2 \propto \vec{\sigma}^{\mp}$ (where $\vec{\sigma}^{\mp} = \vec{e}_x \pm i\vec{e}_y$) in the far field zone. The latter, being the electric fields of the circularly polarized incoming planar waves in the near field zone, can be easily calculated via the optical scattering matrix [16,17]. Averaging the resulting intensities over the random directions of the QD dipole at point $\mathbf{r}$, we get

$$I^{\pm}(\mathbf{r}) \propto \langle|\mathbf{E}_1^{\pm}|^2\rangle \propto |\mathbf{E}_2^{\mp}(\mathbf{r})|^2. \tag{3}$$

Then ρ_c of emission of a randomly oriented (in xy plane) point dipole at point $\mathbf{r}$ can be calculated for any direction via the local xy components of the electric field of a planar wave incoming from the opposite direction as

$$\rho_{c,\mathrm{loc}}(\mathbf{r}) = \frac{|\mathbf{E}_2^-(\mathbf{r})|^2 - |\mathbf{E}_2^+(\mathbf{r})|^2}{|\mathbf{E}_2^-(\mathbf{r})|^2 + |\mathbf{E}_2^+(\mathbf{r})|^2}. \tag{4}$$

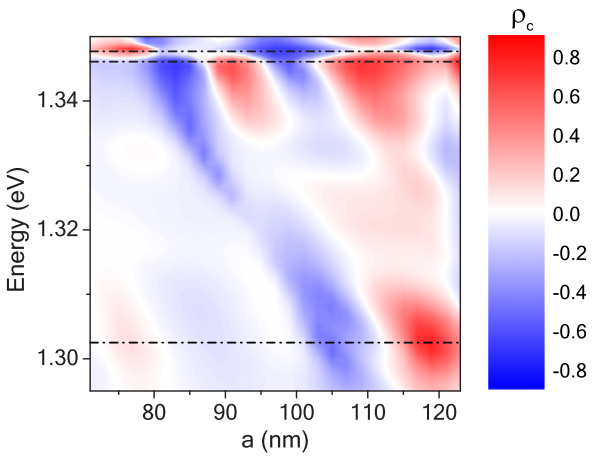

FIG. 4. (Color online) The calculated dependence of the circular polarization degree of emission in the normal to the MC plane direction on the gammadion linewidth a and photon energy, for right gammadions with $L = 400$ nm, period $d = 1000$ nm, and Bragg pairs etching depth $N_{\mathrm{etch}} = 10$. The averaged ρ_c is shown in color; the color scheme is explained in the color bar. The dash-dotted lines show the spectral positions of the lowest QD emission lines in the normal direction.

To calculate ρ_c of emission of all randomly positioned dipoles ρ_c we have to average Eq. (3) over the unit cell,

$$I^{\pm} = \overline{I^{\pm}(\mathbf{r})} \propto \overline{|\mathbf{E}_2^{\mp}(\mathbf{r})|^2}. \tag{5}$$

Finally we arrive at the equation

$$\rho_c = \frac{\overline{|\mathbf{E}_2^-(\mathbf{r})|^2} - \overline{|\mathbf{E}_2^+(\mathbf{r})|^2}}{\overline{|\mathbf{E}_2^-(\mathbf{r})|^2} + \overline{|\mathbf{E}_2^+(\mathbf{r})|^2}}. \tag{6}$$

The emission intensities and circular polarization degrees vs in-plane photon momentum calculated using Eqs. (5) and

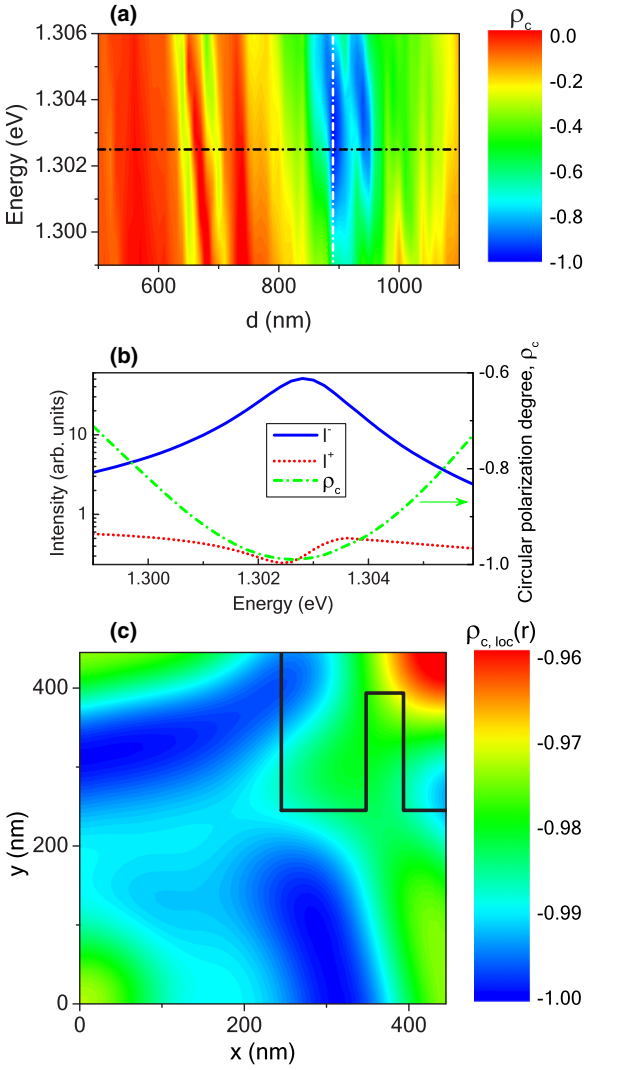

FIG. 5. (Color online) Calculated dependence of the circular polarization degree ρ_c of emission on period d for the structure with $L = 400$ nm, $a = 105$ nm (a). Calculated emission spectra I^+, I^- and circular polarization degree ρ_c for the optimized structure with $d = 890$ nm (b) [white vertical line in panel (a)]. The calculated circular polarization degree $\rho_{c,\mathrm{loc}}(r)$ of emission of a randomly oriented QDs in the optimized structure from a spatial position r in the normal direction at peak photon energy $\hbar\omega = 1.3028$ eV, one fourth of the unit cell of the etching is shown (c). The distribution over the whole unit set can be reconstructed via 90° rotations around the unit cell center in the top right vertex of panel (c), because of C_4 symmetry. Black line in panel (c) shows the position of the right-twisted gammadion-shaped pillar as seen from the MC bottom.

(6) are shown in the right panels of Fig. 3. They are in a qualitative agreement with the experiment, at least for the (0,0) and (±1,0) branches. The calculated intensities are normalized to the maximum emission intensity of the same point dipoles in vacuum, i.e., without the MC. The calculation was made with $15 \times 15 = 225$ spatial harmonics, which provides approximately a 10% accuracy of the simulation. The differences for the (0,±1) and higher branches may be due to a much larger sensitivity of the latter to the details of the real structure geometry, which cannot be properly taken into account in the simulations. In particular, the deviations of the experimental structure (with slightly inclined walls) from the ideal one in the calculation (with vertical walls) can be clearly seen in Fig. 1(b). Additionally, the experimental samples have a slightly broken square symmetry which causes a weak linear polarization of the QDs emission even in the normal direction (not shown).

The simulations show that the circular polarization degree of QD emission depends strongly on the gammadion linewidth a. This behavior is oscillatory. It is illustrated in Fig. 4, for the case of chiral etching through 10 Bragg pairs of the top mirror, period 1000 nm and gammadion size 400 nm.

The calculated dependence of the circular polarization degree on the period is illustrated in Fig. 5(a) for gammadions with $L = 400$ nm, $a = 105$ nm, and an etching depth of 10 Bragg pairs. Note that the averaged circular polarization degree can exceed $|\rho_c| > 98\%$ in the optimized structure with $d = 890$ nm; see the white vertical line in Fig. 5(a) and the corresponding spectral dependencies of $I^{\pm}$ and ρ_c in Fig. 5(b). The spatial distribution of the local circular polarization degree $\rho_{c\mathrm{loc}}$ for the optimized structure at the (0,0) resonance photon energy $\hbar\omega = 1.303$ eV is shown in Fig. 5(c). It is seen that the (0,0) resonance becomes very effective from the point of view of producing the circularly polarized emission. A departure from ideality which is inherent to the present structure with many slightly different gammadions and randomly distributed QDs may make it difficult to reach this high theoretical estimate experimentally. Note, however, that state-of-the-art semiconductor fabrication technology allows a precise control of the cavity structure and the position of the radiation emitters [18,19]. This makes possible even a further optimization of the structure if the QDs are positioned in the dark blue regions around the gammadion [see in Fig. 5(c)] where $\rho_{c,\mathrm{loc}}$ is very close to 1. Thus, provided that a single QD emitter is placed into our structure in a correct place, this system is expected to work as a single photon emitter of circularly polarized light.

In conclusion, we have demonstrated a spatially structured planar MC system fabricated from achiral semiconductor materials that ensures left-right circular polarization asymmetry of the electromagnetic modes. The imbalance between left- and right-circular polarization of the QD emitted light in the demonstrated structure results in a degree of the circular polarization as high as 81% for zero magnetic field—this is in agreement with theoretical simulations. Theoretical optimization has shown that a polarization degree exceeding 98% can be obtained in optimized structures with random positioning of quantum dots. This can be increased to close to 100% when the positions of the QD are controlled in the structure. The aforementioned possibility of making a single photon emitter of circularly polarized light due to the precise control of the cavity structure and the QD position [18,19] is hardly achievable in a conventional system of dyes in chiral liquid crystals. All together, these possibilities make the chiral spatially structured planar semiconductor MCs useful for various applications in nanophotonics, including quantum information technology.

This work was supported by EU project SPANGL4Q and RFBR Project No. 13-02-12144. We are grateful to K. Konishi, L. Kuipers, M. Kuwata-Gonokami, R. Oulton, H. Tamaru, and T. Weiss for fruitful discussions, and to Todd Meyrath for a critical reading of the manuscript.

[1] E. Yablonovitch, Phys. Rev. Lett. **58**, 2059 (1987).
[2] S. Fan, P. R. Villeneuve, J. D. Joannopoulos, and E. F. Schubert, Phys. Rev. Lett. **78**, 3294 (1997).
[3] E. Miyai, K. Sakai, T. Okano, W. Kunishi, D. Ohnishi, and S. Noda, Nature (London) **441**, 946 (2006).
[4] J. P. Reithmaier, G. Sek, A. Loffler, C. Hofmann, S. Kuhn, S. Reitzenstein, L. V. Keldysh, V. D. Kulakovskii, T. L. Reinecke, and A. Forchel, Nature (London) **432**, 197 (2004).
[5] D. Englund, D. Fattal, E. Waks, G. Solomon, B. Zhang, T. Nakaoka, Y. Arakawa, Y. Yamamoto, and J. Vučković, Phys. Rev. Lett. **95**, 013904 (2005).
[6] K. Konishi, M. Nomura, N. Kumagai, S. Iwamoto, Y. Arakawa, and M. Kuwata-Gonokami, Phys. Rev. Lett. **106**, 057402 (2011).
[7] L. D. Barron, Nature (London) **238**, 17 (1972).
[8] M. Kuwata-Gonokami, N. Saito, Y. Ino, M. Kauranen, K. Jefimovs, T. Vallius, J. Turunen, and Y. Svirko, Phys. Rev. Lett. **95**, 227401 (2005).
[9] K. Konishi, B. Bai, X. Meng, P. Karvinen, J. Turunen, Y. P. Svirko, and M. Kuwata-Gonokami, Opt. Express **16**, 7189 (2008).
[10] G. Panzarini, L. C. Andreani, A. Armitage, D. Baxter, M. S. Skolnick, V. N. Astratov, J. S. Roberts, A. V. Kavokin, M. R. Vladimirova, and M. A. Kaliteevski,Phys. Solid State **41**, 1223 (1999).
[11] D. M. Whittaker and I. S. Culshaw, Phys. Rev. B **60**, 2610 (1999).
[12] D. M. Whittaker, Opt. Lett. **25**, 779 (2000).
[13] H. Taniyama and M. Notomi, J. Appl. Phys. **103**, 083115 (2008).
[14] S. V. Lobanov, T. Weiss, D. Dregely, H. Giessen, N. A. Gippius, and S. G. Tikhodeev, Phys. Rev. B **85**, 155137 (2012).
[15] L. D. Landau, L. P. Pitaevskii, and E. M. Lifshitz, *Electrodynamics of Continuous Media, Second Edition: Vol. 8* (Elsevier, Amsterdam, 1984), Chap. 89.
[16] S. G. Tikhodeev, A. L. Yablonskii, E. A. Muljarov, N. A. Gippius, and T. Ishihara, Phys. Rev. B **66**, 045102 (2002).
[17] T. Weiss, G. Granet, N. A. Gippius, S. G. Tikhodeev, and H. Giessen, Opt. Express **17**, 8051 (2009).
[18] A. Dousse, L. Lanco, J. Suffczyński, E. Semenova, A. Miard, A. Lemaître, I. Sagnes, C. Roblin, J. Bloch, and P. Senellart, Phys. Rev. Lett. **101**, 267404 (2008).
[19] C. Schneider, T. Heindel, A. Huggenberger, P. Weinmann, C. Kistner, M. Kamp, S. Reitzenstein, S. Höfling, and A. Forchel, Appl. Phys. Lett. **94**, 111111 (2009).